

ATMOSPHERIC EFFECTS ON CRATERING EFFICIENCY; P.H. Schultz, Brown University, Dept. of Geological Sciences, Providence, RI 02912

Introduction: The presence of an atmosphere can affect cratering efficiency (displaced target mass in projectile masses) through at least three processes: static atmospheric overpressure (P_0) adding to the lithostatic overburden; dynamic pressure acting on ejecta (P_e); and changes in coupling due to projectile-atmosphere interactions. Separation of these three processes are difficult because they involve many of the same controlling variables. Previous studies reported the possible roles of static atmospheric pressure (1, 2) and dynamic pressure (3). Observed contradictions with earlier studies (1) and systematic departures within new data (3), however, required assessing the potential effects of projectile-target interactions. This contribution reviews the relative role of the three processes based on laboratory experiments designed to isolate their effects for cratering in particulate targets.

Experimental Approach: The impact experiments were performed with the NASA-Ames Vertical Gun, a facility uniquely suited for exploring the role of an atmosphere on gravity-controlled crater growth. Different combinations of environmental (atmosphere), target, and impactor variables permitted resolving the three controlling processes. The role of static atmospheric pressure can be isolated by minimizing the effects of both dynamic pressure and projectile-atmosphere interaction. With a working model of the independent variables controlling static pressure, the number of experiments also can be reduced by examining the effects at a given value of the assumed controlling parameter. The present analysis followed the approach of Holsapple (1) who proposed that static atmospheric pressure can be described by a dimensionless parameter comparing ambient pressure (P) with bulk target density (δ) multiplied by the specific energy Q , i.e., $1/2v^2$ for impact velocity of v . This approach was shown to be equivalent to the more classical description where atmospheric pressure adds to the lithostatic overpressure, thereby changing the effective depth of burst (1). This approach also indicated, however, that atmospheric pressure has little effect on cratering efficiency.

Results: The effect of P_e was minimized by the use of an atmosphere with low density (helium) and ejecta with large sizes (coarse sand). The potential effect of projectile-atmosphere interactions also was minimized by using helium (high mach number) and low impact velocities (2 km/s). Figure 1 summarizes these results and reveals that ambient atmospheric pressure alone reduces cratering efficiency with $(P/\delta v^2)$ raised to a power law of $-\beta \simeq -0.23$ for both pumice and fine sand targets.

Dynamic pressure effects can be expressed in terms of a dimensionless drag parameter (d/g) where drag deceleration, d , is scaled to gravitational acceleration, g (4, 5). Such effects can be explored simply by expressing the data in terms of this ratio, but it is more useful to view it as a modification to the π_2 parameter as gravity-controlled growth becomes drag-controlled growth for $d \gg g$. The observed cratering efficiencies were corrected for P_0 using the exponent derived above and then plotted against (d/g) . Three different expressions for (d/g) can be given for contrasting environmental and target conditions. First, the small ejecta size ($a \sim 85\mu$) and low ejection velocities (50–100 cm/s) at late stages for a pumice target result in a drag coefficient that varies inversely proportional to the Reynolds number, Re . It can be shown that the resulting expression for (d/g) for a given target simply depends on μv_e where μ is the viscosity of the ambient atmosphere; this also can be expressed as $\mu R_v^{1/2}$ where R_v is the radius of the crater had it formed in a vacuum through scaling relations (5, 6). Second, conditions leading to a narrow range of Re result in a constant drag coefficient; hence (d/g) can be shown to vary with ρR_v for a given target where ρ is the ambient atmospheric density. And third, targets with different size ejecta should result in (d/g) varying as $\mu R_v/a^2$ if the drag coefficient is inversely proportional to the Re . Figure 2 illustrates this third approach. All three approaches indicated that drag affects cratering efficiency with the same exponent, $-\alpha$, as g in the π_2 parameter for vacuum conditions.

The data were tested for consistency by plotting cratering efficiency corrected for P_0 and P_e against the Reynolds number. If the approach taken was valid and if no other processes were involved, then the ordinate becomes the inverse of the drag coefficient, and the data should show no systematic variations. Systematic departures dependent on atmospheric composition, however, did emerge. Moreover, augmentation (rather than reduction) in cratering efficiency was consistently observed under certain conditions, and the results for P_0 still conflicted with previous studies (1). These observations required exploring alternative approaches for relevant scaling parameters as well as possible clues for other controlling processes.

High-frame photography clearly revealed a bright ionized wake trailing the impactor at high velocities (>4 km/s) and ambient pressures (>0.5 bars) that appeared to modify crater formation (7). New experiments were designed to separate the projectile from its wake, thereby establishing its possible role in crater excavation. This approach revealed two effects. At lower mach numbers (<6) and ambient pressures (<0.5 bars), the wake is injected into the growing cavity created by the projectile and adds a backpressure (Figure 3). Stagnation pressure created by hypervelocity impingement of a gas jet on particulate surfaces (8) provided an expression for this backpressure as $P_0 \gamma M^2 (\gamma - 1)$ where M is mach number and γ is the ratio of specific heats for the gas. This backpres-

sure augments cratering efficiency with a power-law exponent identical to but opposite in sign, to ambient pressure effects. Hence, collision by the projectile wake can be viewed as a process decoupled from the projectile. The observed offsetting effects of backpressure and ambient pressure may provide an explanation for previous studies (1) indicating minimal ambient pressure effects. With increasing mach numbers and pressures, however, cratering efficiency once again decreases. On the basis of previous experience with clustered impacts (9), low-density collisions have little effect on cratering efficiency if referenced to the cluster diameter. Hence the projectile wake at high mach numbers and ambient pressures was assumed to be coupled to the projectile, thereby increasing the projectile radius, r_p , to an effective radius, r_e . The resulting expression was found to accommodate the data with an exponent equivalent to $-\alpha$.

Concluding Remarks: The effect of an atmosphere on cratering efficiency in particulate targets at laboratory scales can be separated into three dimensionless pressure parameters (ambient, dynamic, and wake pressures) that can be expressed formally in terms of previously derived scaling parameters for gravity-controlled crater growth. It can be shown that ambient pressure should not affect cratering efficiency on the Earth and present-day Mars but could be very different on Venus. The effect of aerodynamic drag, however, could be important with (or producing) fine-size ejecta (see 10). Potential projectile wake effects have been previously explored for Venus in terms of a strong atmospheric blast (11). From the experimental results, here, it is possible that the wake modifies overall coupling at impact and could result in crater shapes and morphologies unique to Venus.

References: (1) Holsapple, K.A. (1980) In *Proc. Lunar Planet. Sci.* 11th, 2379-2401, Pergamon, N.Y. (2) Schultz, P.H. and Gault, D.E. (1982) *Lunar and Planet. Sci.* XIII, LPI, Houston, 694-695. (3) Schultz, P.H. (1988) *Lunar and Planet. Sci.* XIX, LPI, Houston, 1039-1040. (4) Tauber, M.E. et al. (1978) *Icarus* 33, 529-536. (5) Schultz, P.H. and Gault, D.E. (1979) *J. Geophys. Res.* 84, 7669-7687. (6) Housen, K.R. et al. (1983) *J. Geophys. Res.* 88, 2485-2499. (7) Schultz, P.H. and Gault, D.E. (1982) *Geol. Soc. Amer. Sp. Paper* 190, 153-174. (8) Land, N.S. and Clarke, L.V. (1965) NASA TND-2633. (9) Schultz, P.H. and Gault, D.E. (1985) *J. Geophys. Res.* 90, 3701-3732. (10) Schultz, P.H. (1990) *Lunar and Planet. Sci.* XXI, LPI, Houston (this volume). (11) Ivanov, B.A. et al. (1988) *J. Geophys. Res.* 91, (B4), D413-430.

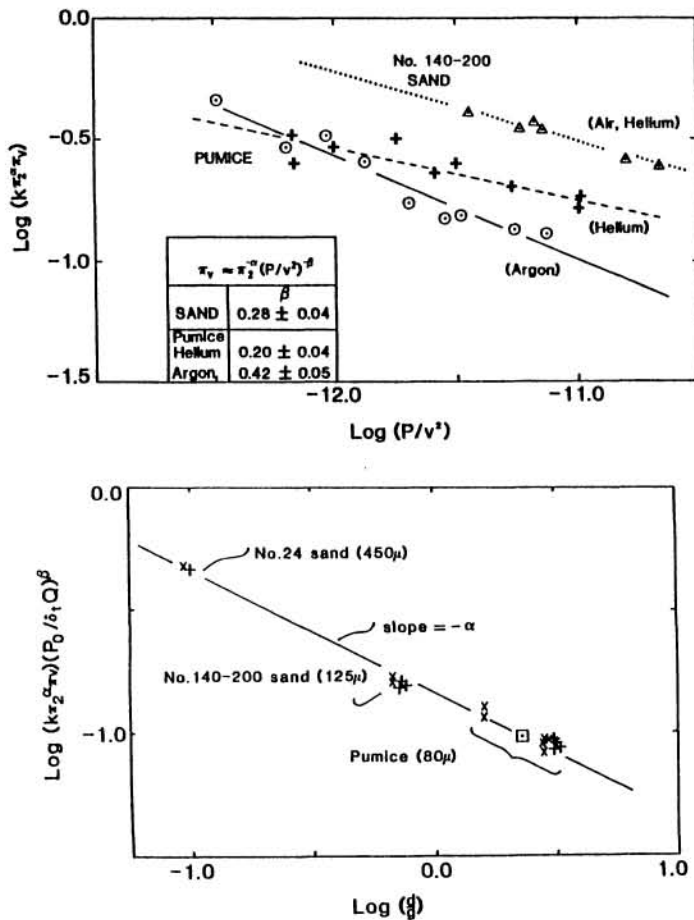


Figure 2. Effect of aerodynamic drag on cratering efficiency (π_v) corrected for gravity (π_2) and ambient pressure ($P/6Q$) where Q is the specific energy ($1/2v^2$). Drag deceleration (d) is scaled to gravitational acceleration (g) and shown for targets with different particle sizes. The resulting exponent, $-\alpha$, for drag-controlled scaling is the same as for gravity-controlled scaling.

Figure 1. Effect of atmospheric pressure of different densities on cratering efficiency (π_v) corrected for gravity scaling (π_2) for compacted pumice targets. Atmospheric pressure (P_0) is incorporated in a dimensionless scaling parameter ($P_0/\delta v^2$) incorporating bulk target density, δ , and impact velocity, v . Here, density has not been included in order to separate data more clearly. Low-density helium atmosphere exhibits a clear effect on cratering efficiency with high-density argon indicating additional processes.

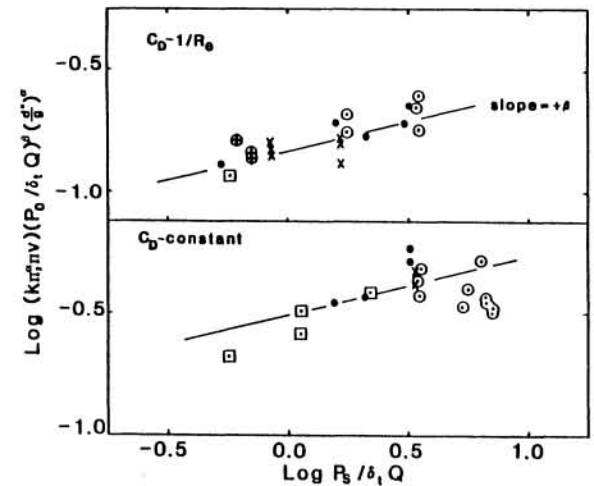


Figure 3. Effect of wake stagnation backpressure (P_w) on cratering efficiency (π_v) corrected for dimensionless scaling parameters for gravity (π_2), ambient pressure ($P_0/6Q$), and drag pressure (d/g). The top half shows a broad range of Reynolds numbers (R_e), where the bottom restricts the range in R_e . Backpressure created by the projectile wake appears to offset ambient pressure effects with the same exponent, β . At high Reynolds numbers, this trend is reversed due to direct coupling with energy/momentum transfer by the projectile.